INFLUENCE OF SURFACE MODIFICATION PARAMETERS ON THE PROPERTIES OF THE Ti-13Zr-13Nb ALLOY FOR IMPLANT APPLICATIONS

Patrycja Głazik[1], Lidia Nowak[1], Dominika Zawisza[1], Zofia Szwałek[1], Jakub Łyko[1], Anna Ronowska[2], Michał Bartmański[1]*

[1] Faculty Of Mechanical Engineering And Ship Technology, Gdańsk University Of Technology, Narutowicza 11/12, 80-233 Gdańsk, Poland
[2] Department Of Laboratory Medicine, Medical University Of Gdansk, M. Skłodowskiej-Curie 3a, 80-210 Gdańsk, Poland

* e-mail: michal.bartmanski@pg.edu.pl

Abstract

Surface modification of titanium alloys constitutes one of the key development directions of modern biomaterials used in orthopedic and dental implantology. This study presents the results of investigations into the influence of parameters of a two-step surface modification of the Ti-13Zr-13Nb alloy, including micro-arc oxidation (MAO) and electrophoretic deposition (EPD), on the properties of the obtained surface layers. The MAO process was carried out for 5 and 10 minutes in an electrolyte containing calcium and phosphorus compounds. Subsequently, a nanohydroxyapatite coating with the addition of silver nanoparticles was deposited on the modified surfaces using the EPD method. The obtained samples were subjected to comprehensive characterization, including Vickers microhardness measurements, evaluation of coating thickness and uniformity, analysis of surface morphology and chemical composition (SEM/EDS), wettability and surface free energy measurements, coating adhesion tests, and cell studies. The results demonstrated a significant increase in microhardness and surface hydrophilicity after MAO–EPD modification compared to the reference material. The obtained Ca/P ratio was close to that of natural bone, indicating the bioactive potential of the produced layers. Indirect cytotoxicity testing revealed that EPD-modified surfaces and MAO (10 min) combined with EPD were non-cytotoxic, maintaining viability above 90. In contrast, MAO (5 min) + EPD extracts significantly reduced cell viability to approximately 65–70%. The MAO 5 min + EPD variant achieved other favorable properties, as it exhibited good uniformity, high microhardness, and acceptable coating adhesion. The results confirm the validity of applying the two-step surface modification of the Ti-13Zr-13Nb alloy in the design of bioactive implant surfaces.

Keywords: *titanium alloy, micro-arc oxidation, electrophoretic deposition, nanohydroxyapatite, nanosilver*

[Engineering of Biomaterials 174 (2026) 11]

doi:10.34821/eng.biomat.174.2026.11

Submitted: 2026-05-10, Accepted: 2026-06-15, Published: 2026-06-19

Introduction

Titanium alloys are widely used in orthopedic and dental implantology, and constitute a preferred group of materials for biomedical applications due to their excellent biocompatibility and favorable mechanical properties [1-4]. Implants made of titanium and its alloys are extensively applied in clinical practice; however, despite their high material potential, limitations related to the interaction between the implant surface and the surrounding tissue still remain [1]. Titanium owes its widespread biomedical application to its high corrosion resistance in physiological environments, good mechanical strength, and the ability to form a stable passive oxide layer on its surface [4]. However, this naturally formed TiO_2 layer is biologically inert and does not actively stimulate bone tissue response [4]. One of the key problems associated with metallic implants is the bioinert nature of titanium surfaces. Despite good bulk properties, Ti alloy surfaces often exhibit limited bioactivity, which may hinder close integration of the implant with surrounding tissues and affect the long-term success of implantation [1,5].

This phenomenon provides a strong rationale for the development of surface engineering methods aimed at improving material–tissue interactions and enhancing the bioactivity of titanium implant surfaces. Another clinically significant issue is the mismatch between the mechanical properties of the implant and those of bone tissue. The difference between the high elastic modulus of conventional titanium alloys and the much lower modulus of bone may lead to the phenomenon known as stress shielding, resulting in bone resorption and an increased risk of implant loosening [6]. The elastic modulus of conventional titanium alloys significantly exceeds that of cortical bone, leading to non-physiological load transfer and the stress shielding effect [6]. In this context, particular attention has been focused on β-type titanium alloys, which are characterized by a reduced Young's modulus and are considered beneficial materials for limiting bone loss and improving bone remodeling [6-8]. The reduction of the elastic modulus in β-type titanium alloys is achieved through the addition of non-toxic β-phase stabilizing elements, such as niobium and zirconium [6]. Among modern β-type titanium alloys intended for biomedical applications is the Ti-13Zr-13Nb alloy, which was developed as an alternative to conventional implant alloys.

The presence of niobium and zirconium as β-phase stabilizing elements allows this material to be classified as an alloy with a potentially reduced elastic modulus and improved mechanical compatibility with bone tissue, consistent with general trends in the development of metallic biomaterials reported in the literature [6,9]. For this reason, the Ti-13Zr-13Nb alloy has become the subject of intensive research in the context of implant applications [10]. Despite favorable bulk properties, the surface of Ti-13Zr-13Nb remains bioinert, similarly to other titanium alloys, which necessitates the use of surface modification techniques [5]. Due to the simultaneous occurrence of surface bioinertness and the need to enhance implant–bone interactions, surface modification methods of titanium alloys are of particular importance.

Among these methods, electrochemical techniques such as micro-arc oxidation (MAO) have attracted considerable interest, as they enable the formation of porous oxide layers strongly bonded to the metallic substrate and allow the incorporation of electrolyte components into the coating structure [1,5]. Compared to conventional anodizing, the MAO process enables the formation of thicker and more porous oxide layers, which are beneficial for bone ingrowth and mechanical stability [5]. The MAO process offers significant

potential for creating bioactive layers on titanium implants, making it a promising surface modification technique also for β-type titanium alloys, including Ti-13Zr-13Nb [5]. The porous structure formed during MAO creates favorable conditions for subsequent electrophoretic deposition (EPD) of bioactive coatings, enabling mechanical anchoring of deposited layers within the oxide structure [2].

Materials and methods

Sample Preparation

Cylindrical samples of the Ti-13Zr-13Nb titanium alloy (Sea-Bird Metal Materials Co., Baoji, China), with a diameter of 20 mm and a thickness of 4 mm, were prepared by grinding using abrasive papers with grit sizes of 220, 500, and 800. Reference samples consisted of the material in its initial condition (after grinding but prior to the MAO and EPD processes) and were used as a baseline for comparison with the modified surfaces.

Micro-Arc Oxidation Process

The micro-arc oxidation (MAO) process was performed at a constant voltage of 300 V and current of 83 mA (selected based on the study [37]), for 5 and 10 minutes, respectively. A total of 250 mL of electrolyte containing 0.1 M calcium glycerophosphate (TCI) and 0.15 M calcium acetate (Chempur) was used. The same electrolyte was used for three samples during the process. The experiment was conducted using an MAO setup equipped with a DC power supply (PL-650-0.1, Matsusada Precision INC., Japan), a magnetic stirrer, and a glass electrolyte vessel cooled with water to maintain room temperature conditions. The electrolyte was stirred at a speed of 200 rpm using a magnetic stirrer. The titanium alloy sample served as the anode, while a stainless-steel plate acted as the cathode. Only one side of each sample was subjected to the MAO process, while the opposite side remained unmodified. After completion of the process, the samples were rinsed with distilled water and dried.

Electrophoretic Deposition

The subsequent stage of surface modification involved electrophoretic deposition (EPD) of a coating onto samples previously treated by the MAO process. The EPD process was carried out in a colloidal suspension composed of 0.1 g of hydroxyapatite nanopowder (Sigma Aldrich, St. Louis, MO, USA) and 0.005 g of silver nanoparticles with a particle size of 30 nm (Hongwu International Group Ltd., Guangzhou, China), dispersed in 100 mL of 96% ethanol (C_2H_5OH). The EPD process was performed at room temperature under a constant voltage of 30 V for 2 minutes. The system consisted of the sample acting as the cathode and a platinum electrode serving as the anode. After a 24-hour waiting period, the samples were sintered in a laboratory furnace at 800ºC for 2 hours at vacuum in order to consolidate the coating and improve its adhesion to the porous titanium substrate.

Scanning Electron Microscopy (SEM) and Energy-Dispersive X-ray Spectroscopy (EDS)

Surface morphology and microstructure of the samples were examined using a high-resolution scanning electron microscope (SEM JEOL JSM- 7800 F, JEOL Ltd, Tokyo, Japan). The chemical composition was determined using energy-dispersive X-ray spectroscopy (EDS) with a detector integrated into the scanning electron microscope (SEM) with an accelerating voltage of 20kV and spot analysis.

Coating Thickness Measurements

Coating thickness measurements were performed using an Isoscope-type coating thickness gauge (FMP10-20, Helmut Fischer GmbH, Sindelfingen, Germany). For each group of coated samples, measurements were conducted on two samples, and 20 measurements were carried out at randomly selected locations. Each measurement was conducted by placing the probe directly onto the surface of the coated titanium sample.

Vickers Microhardness Testing

Microhardness measurements were performed using the Vickers method with a load of 50 g. A hardness tester manufactured by AFFRI TESTING INSTRUMENTS was used.

Wettability Measurements

Wettability measurements were performed using a goniometer (Theta Lite TL101, Biolin Scientific) employing the sessile drop method. Measurements were carried out using two test liquids: distilled water and diiodomethane. The volume of the distilled water and diiodomethane droplets was approximately 2 µL, and the contact angle was recorded for 10 s after the droplet was deposited on the surface.

Surface Free Energy Determination

Surface free energy and its polar and dispersive components were calculated based on the measured contact angle values obtained for distilled water and diiodomethane.

Adhesion Test

Adhesion of the deposited coatings to the titanium substrate was evaluated using a cross-hatch scratch test. The test was performed using an Elcometer 107 Cross Hatch Cutter Full Kit with ISO tape (6 × 1 mm cutter), Part Number F10713348-6. The results were evaluated according to the ISO 2409 classification.

Cells studies

For the cell culture experiments, the cellular model consisted of human osteoblasts hFOB 1.19 (RRID: CVCL_3708) obtained from ATCC. Cells were cultured in a 1:1 mixture of Ham's F12 medium and Dulbecco's Modified Eagle's Medium (without phenol red), supplemented with 1 mmol/L L-glutamine, 0.3 mg/mL G418, and 10% fetal bovine serum. Cells used for the experiments were between passages 5 and 8 and were passaged twice prior to each experiment. The cultures were maintained at 34°C in a humidified atmosphere containing 5% CO_2 and 95% air. To assess the indirect effects of the tested materials, cells were exposed to medium preconditioned with the tested samples. Cells were seeded in 96-well plates at a density of 0.012 mln per well and cultured under standard conditions for 24 h. The culture medium was then replaced with extracts of the test materials, and incubation continued for an additional 24 h. Cell viability was evaluated using the MTT reduction assay (3-[4,5-dimethylthiazol-2-yl]-2,5-diphenyltetrazolium bromide), which measures mitochondrial enzymatic activity, primarily succinate dehydrogenase. MTT solution (0.06 mmol/L) was added to the cells remaining attached to the tested surfaces, followed by incubation for 4 h to allow for dye metabolism. The resulting formazan product was measured spectrophotometrically at 570 nm. Control cells were cultured on unmodified samples.

Statistic

The results are presented as means ± standard deviations (SD), and the obtained relationships were evaluated using one-way ANOVA followed by Tukey's True Significant Difference post hoc test, with statistical significance set at $p < 0.05$. The normality of the data distribution was verified using the Shapiro–Wilk test. All statistical analyses were performed using GraphPad Prism 10 (GraphPad Software, La Jolla, CA, USA).

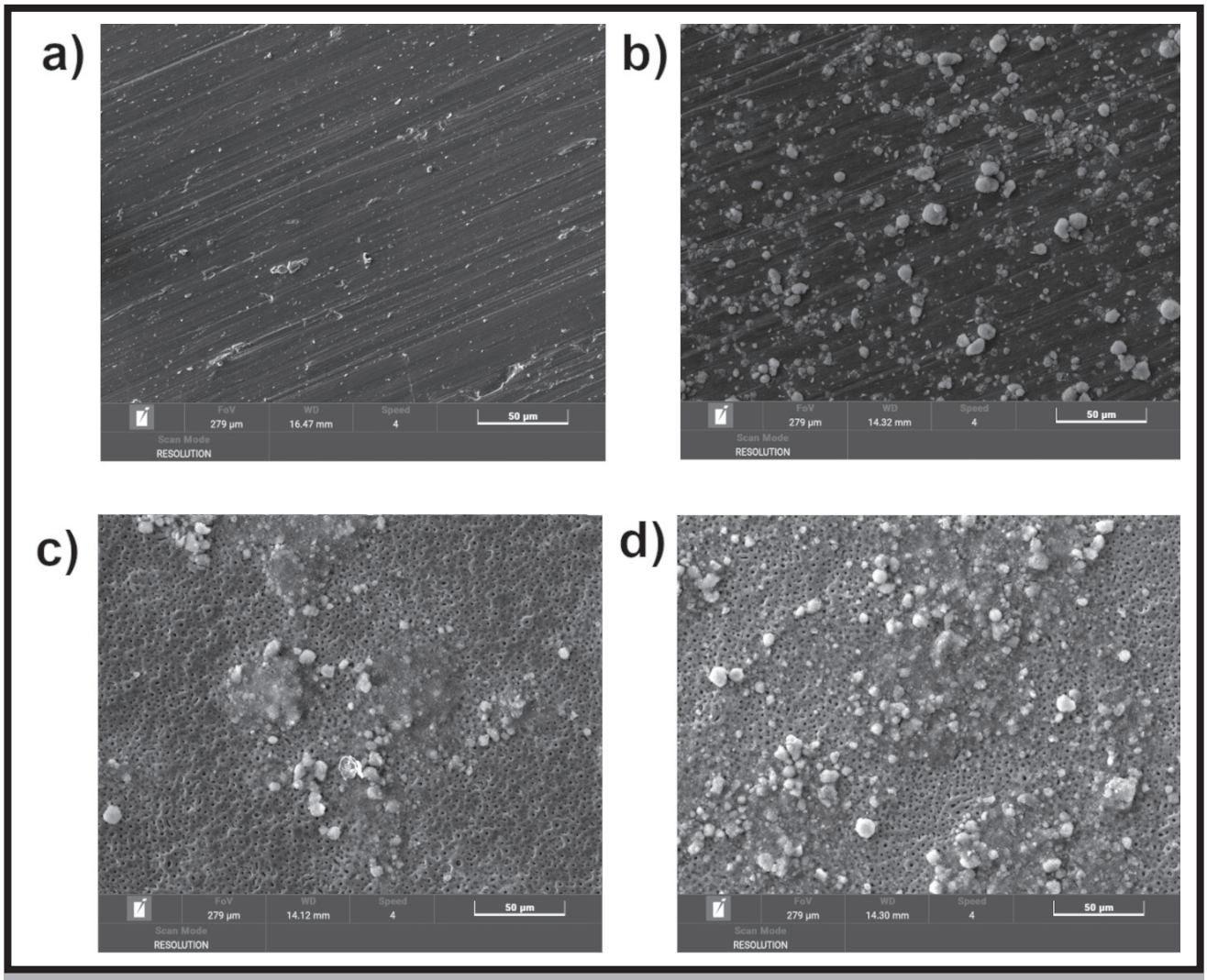

FIG. 1. Microstructure of the a) reference sample; b) reference + EPD sample; c) MAO 5 min + EPD sample; d) MAO 10 min + EPD sample, magnification 1000

Results and discussion

Surface microstructure and chemical composition analysis

Analysis of the microscopic images revealed clear morphological differences between the reference sample and samples subjected to MAO and EPD processes, resulting from different mechanisms of surface layer formation (FIG. 1). The surface of the reference sample after mechanical treatment was characterized by the presence of numerous parallel grinding marks resulting from the action of abrasive paper grains. No porosity typical of electrochemical processes was observed; only minor irregularities and local contaminations related to the final stage of substrate preparation were present. In the case of the reference sample after the EPD process, the surface of the metallic substrate remained essentially smooth, with clearly visible traces of mechanical grinding. The EPD process resulted in the deposition of agglomerates of hydroxyapatite nanopowder and silver nanoparticles, which were distributed unevenly on the surface. The absence of a porous underlayer caused these particles to adhere directly to the flat metallic surface, without anchoring within the substrate structure. Significant changes in surface morphology were observed for samples subjected to the micro-arc oxidation process. For the MAO 5 min + EPD variant, a developed, porous surface structure characteristic of the MAO process was identified. The coating exhibited a uniform network of micropores with sizes ranging from fractions of a micrometer to several micrometers. Particles deposited during the EPD process were visible as bright regions, which appeared to be located within the porous depression as well as on the tops of the oxide layer. Extending the MAO process time to 10 minutes affected the density and size of the pores while maintaining the porous character of the surface. The obtained layer was well consolidated and did not exhibit visible thermal cracks, which indicates the stability of the process and good quality of the obtained coating.

EDS analysis (FIG. 2) revealed the presence of elements characteristic of the investigated Ti-13Zr-13Nb alloy, i.e., Ti, Zr, and Nb, as well as oxygen, calcium, and phosphorus in samples subjected to electrochemical modification. In the case of samples after the MAO process, a distinct increase in oxygen content exceeding 40 wt.% was observed, which confirms the formation of a stable oxide layer during anodization. The simultaneous detection of alloying elements indicates their migration from the metallic substrate into the forming surface layer. The presence of calcium and phosphorus in the layers formed after the MAO process indicates effective incorporation of these elements into the coating structure from the electrolyte containing calcium glycerophosphate and calcium acetate. Based on the EDS results, an atomic Ca/P ratio was calculated, amounting to 1.22 for the MAO 5 min + EPD sample and 1.23 for the MAO 10 min + EPD sample. These values are lower than the stoichiometric Ca/P ratio characteristic of hydroxyapatite

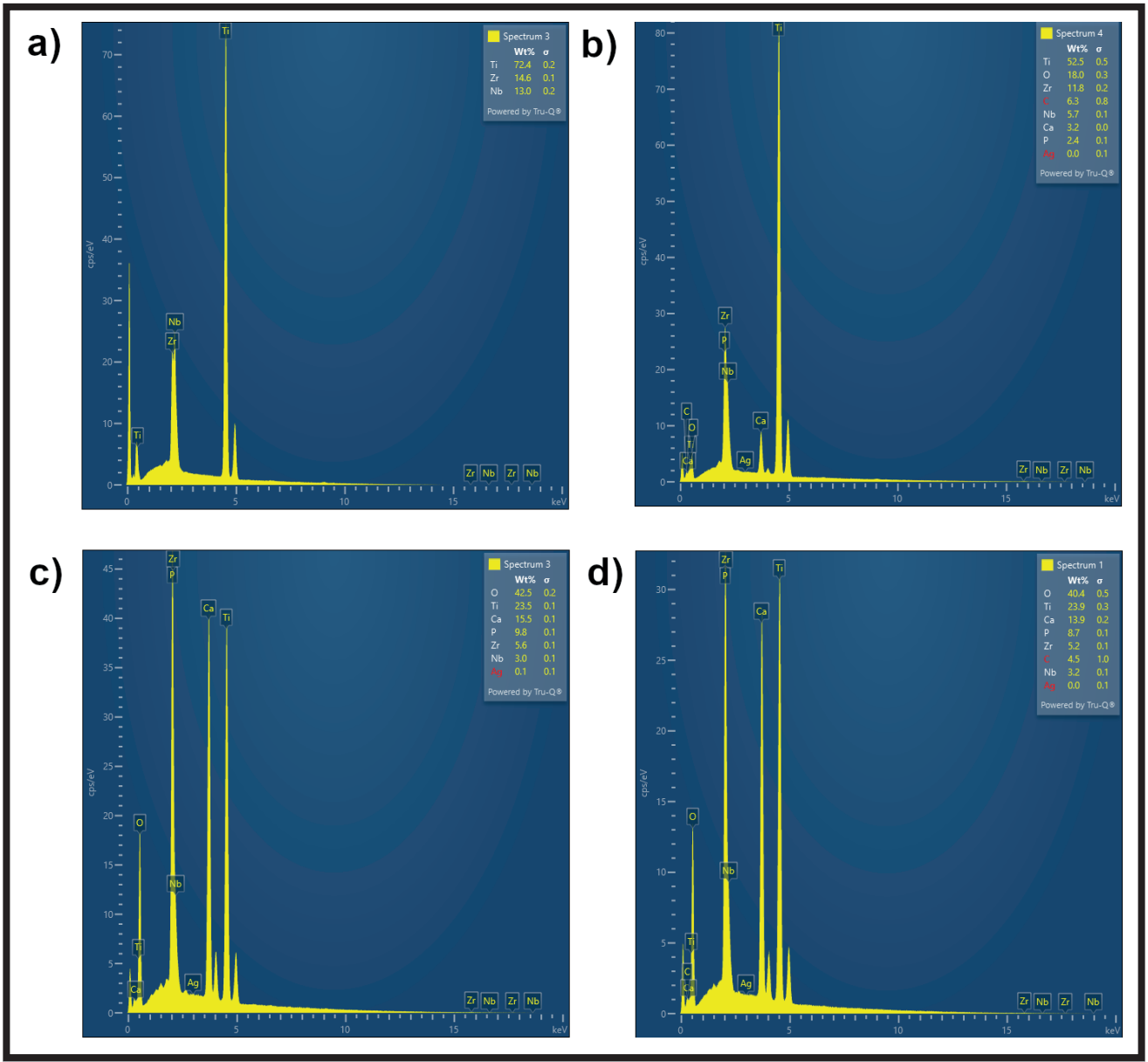

FIG. 2. Elemental composition spectrum of the surface of the a) reference sample; b) reference + EPD sample; c) MAO 5 min + EPD sample; d) MAO 10 min + EPD sample

(1.67), suggesting the formation of calcium phosphates with a reduced Ca/P ratio rather than stoichiometric hydroxyapatite. Despite the introduction of silver nanoparticles during the EPD process, EDS analysis revealed only trace amounts of this element (<1 wt.%). This may result from the low concentration of silver nanoparticles in the suspension, the limited sensitivity of the EDS detector, and possible local agglomeration of nanoparticles outside the analyzed area.

Coating Thickness Measurements and Vickers Microhardness Testing

The thickness was measured at different locations on the sample; therefore, the value of the standard deviation indicates differences in coating thickness depending on the location where the measuring probe was applied. Based on the spectrum (FIG. 2), it can be stated that the highest average coating thickness was observed for samples with an MAO layer. The reference sample exhibits the highest standard deviation, which confirms that preliminary micro-arc oxidation improves the uniformity of the subsequently deposited EPD coating. Results for the coating thickness (FIG. 3a) indicated clear differences between the investigated groups. Both MAO 5 min + EPD and MAO 10 min + EPD samples exhibited a statistically significant increase in coating thickness compared to the reference + EPD sample (****$p < 0.0001$). In addition, a statistically significant difference in coating thickness was observed between the MAO 5 min + EPD and MAO 10 min + EPD variants (**$p < 0.01$).

Microhardness measurements (FIG. 3b) demonstrated a substantial increase in hardness for all samples subjected to the MAO process compared to the reference substrate. The reference sample exhibited the lowest hardness values and the smallest scatter of results, which is characteristic of a bulk alloy without surface layers. In contrast, the reference + EPD sample showed a high standard deviation exceeding 31%, indicating that the coating deposited directly onto a smooth metallic surface without a porous MAO interlayer was non-uniform or locally delaminated during indentation by the Vickers indenter. Samples subjected to the combined MAO and EPD treatments exhibited more than a twofold increase in microhardness compared to the reference material. Although the average hardness values obtained for the MAO 5 min + EPD and MAO 10 min + EPD variants were comparable and no statistically significant difference was observed between these groups, the 5-minute MAO process resulted in lower scatter of results. This indicates

improved reproducibility and suggests that a shorter MAO treatment time provides a more uniform and mechanically stable surface layer.

Contact Angle and Surface Free Energy Measurements

All groups of samples were analyzed, and the results are presented graphically in FIG. 4.

Contact angle measurements of water and diiodomethane (Fig. 4a,b) showed a great degree of surface wettability modification post-surface treatment. However, there was a substantial reduction in water and diiodomethane contact angles post-EPD surface treatment, and further MAO treatment (5 min and 10 min) led to a marked reduction in near-zero values (**p < 0.001, ***p < 0.0001), suggesting high surface energy surfaces to be highly hydrophilic. Comparison between the MAO 5 min + EPD group and the MAO 10 min + EPD showed no statistically significant difference. Total surface free energy (Figure 4c) increased profoundly after the EPD treatment (p < 0.05) and then further after MAO treatment, with a significantly higher value for both MAO groups compared to the reference and reference + EPD groups (**p < 0.0001). Analysis of the surface free

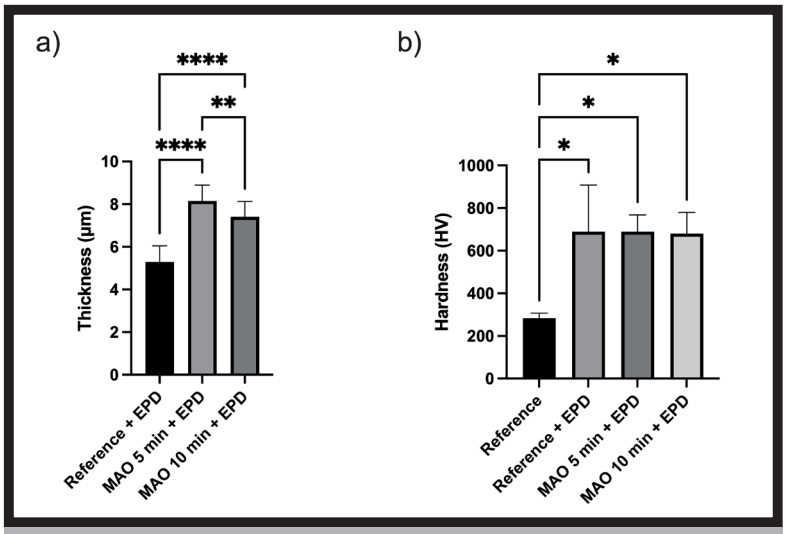

FIG. 3. Thickness (a) and hardness (b) results for tested specimens. Thickness values are presented as mean ± SD from multiple measurements performed at different locations on each sample. Hardness data are presented as mean ± SD from n = 3 independent measurements. Significant differences in hardness were determined by one-way ANOVA followed by Tukey's post hoc test. Statistical significance was indicated as follows: *p < 0.05, **p < 0.01, ***p < 0.001, ****p < 0.0001.

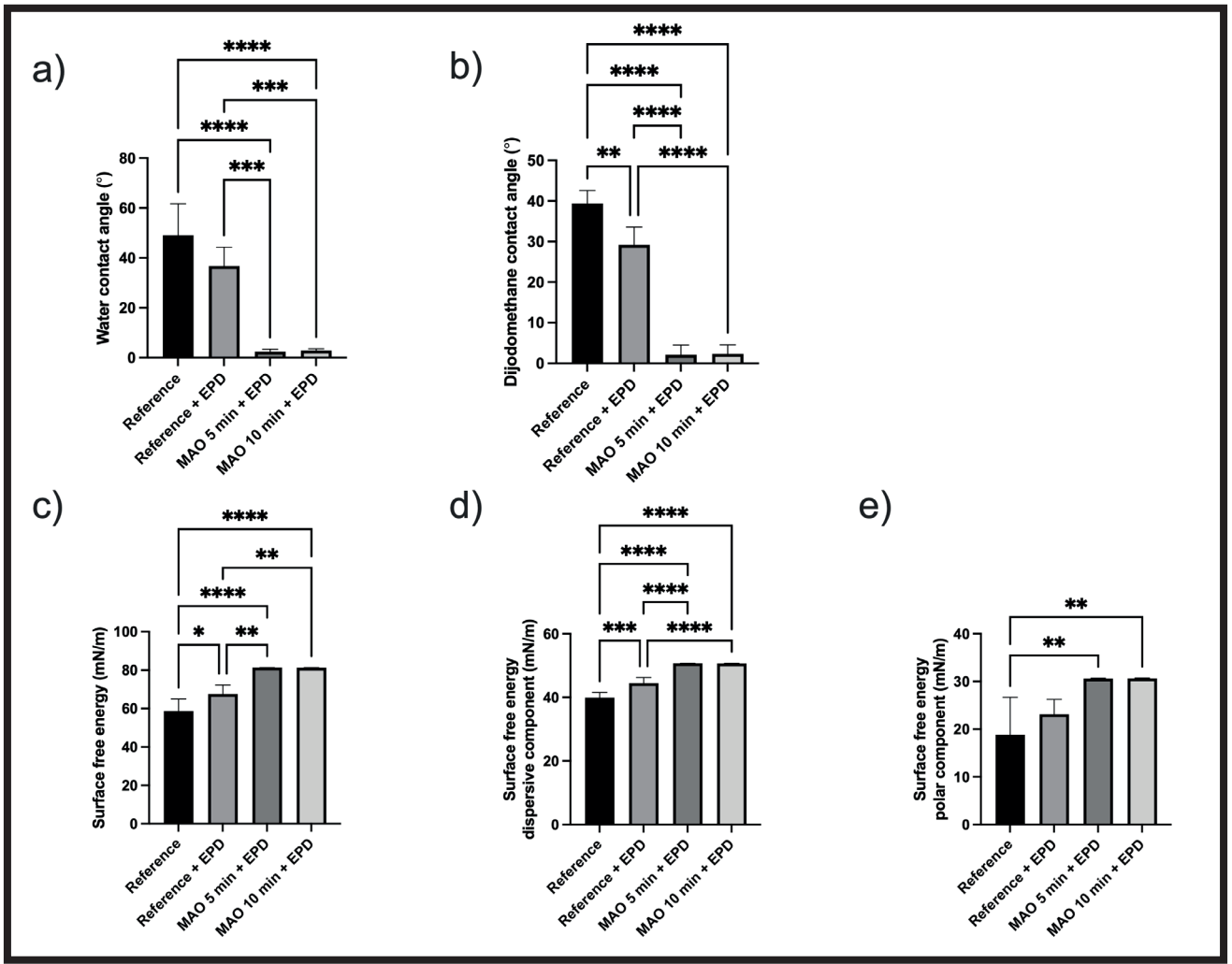

FIG. 4. Water (a) and dijodomethane (b) contact angle results; total surface free energy (c), dispersive component (d) and polar component (e) of teste specimens. Data are presented as means ± SD from n = 4 independent specimens. Significant differences were determined by one-way ANOVA followed by Tukey's post hoc test. Statistical significance was indicated as follows: *p < 0.05, **p < 0.01, ***p < 0.001, ****p < 0.0001.

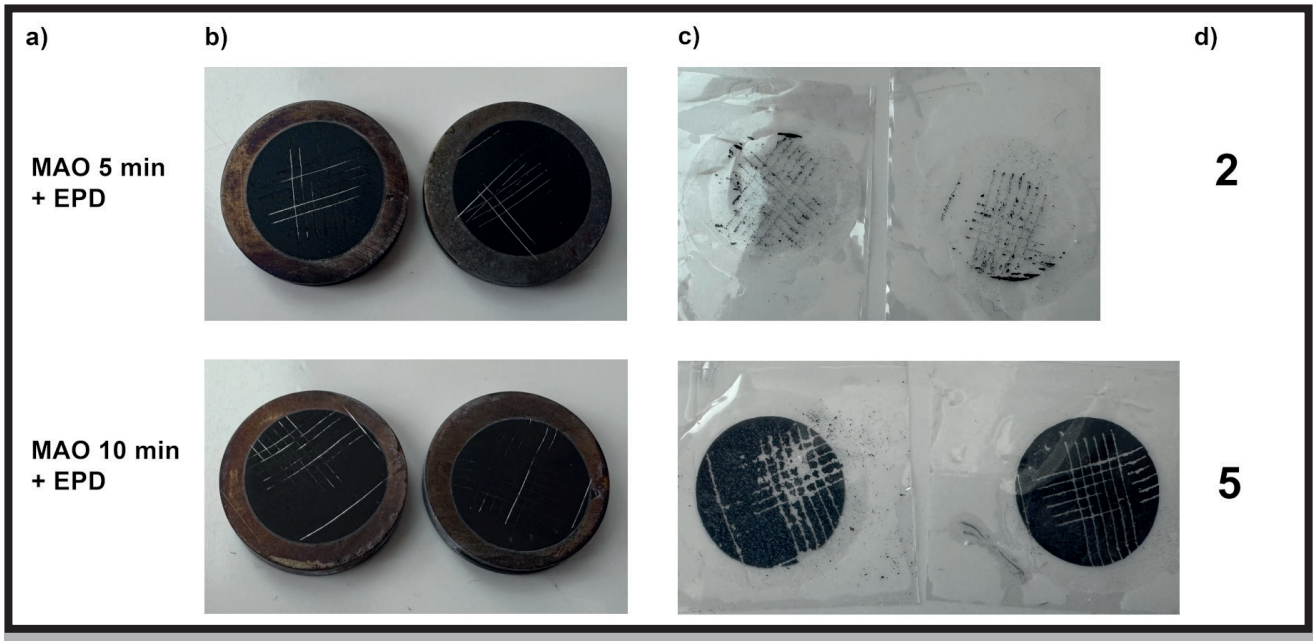

FIG. 5. Samples after the cross-hatch adhesion test a) specimen names, b) surface after cutting, c) tape after tests; d) adhesion class according ISO 2409

energy parameters showed a highly significant increase in both the dispersive (Fig. 4d) and polar (Fig. 4e) parameters following MAO treatment. The dispersive parameter had highly significant differences between the MAO-treated and non-MAO-treated groups (**p < 0.001-***p < 0.0001), while the polar energy increased significantly following MAO treatment (*p < 0.01). There were no significant differences found for the duration of MAO processing.

Scratch Test

The electrophoretically deposited coating applied directly onto the reference substrate exhibited no visible damage after the test, indicating very good adhesion to the substrate and corresponding to the highest adhesion class (ISO 0). The results of the studies interpreted using the comparative method based on the ISO classification are presented on FIG. 5.

In the case of the hybrid coating obtained by combining micro-arc oxidation for 5 min with subsequent EPD deposition, minor chipping localized along the incision lines was observed. The damage was limited and did not extend beyond the immediate vicinity of the cuts, indicating moderate adhesion of the coating to the porous oxide layer. For the MAO 10 min + EPD variant, extensive coating detachment was observed after the test, indicating complete loss of adhesion. The coating was removed over large areas between the cuts, demonstrating insufficient interfacial bonding between the coating and the substrate in this variant. The results indicate that prolongation of the MAO treatment time negatively affects the adhesion of the subsequently deposited EPD coating. Among the investigated variants, the MAO 5 min + EPD treatment provided the most favorable balance between coating development and adhesion to the titanium substrate.

Cells studies

The indirect contact assay performed using hFOB 1.19 osteoblasts revealed no cytotoxic effects for the reference material and samples modified by EPD alone, as cell viability remained close to the control level (100%) (FIG. 6). Similarly, extracts obtained from samples subjected to MAO for 10 min followed by EPD treatment did not significantly affect osteoblast viability, indicating good cytocompatibility. In contrast, a significant reduction in cell viability was observed for extracts from samples treated by MAO for 5 min combined with EPD, with viability decreasing to a range 65–70% of the control. According to ISO 10993-5, materials inducing a reduction in cell viability below 70% are considered to exhibit cytotoxic potential. Therefore, the MAO 5 min + EPD condition demonstrated a borderline to cytotoxic response, while all other tested materials met the criteria for non-cytotoxicity.

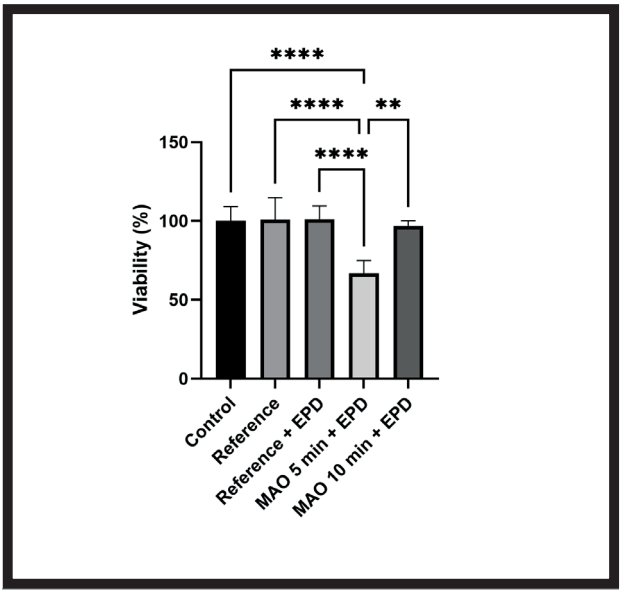

FIG. 6. The effect of tested materials on cells viability. Data are presented as means ± SD from n = 3 independent specimens. Significant differences were determined by one-way ANOVA followed by Tukey's post hoc test. Statistical significance was indicated as follows: *p < 0.05, **p < 0.01, ***p < 0.001, ****p < 0.0001.

Discussion

The application of the two-step modification led to a more than two-fold increase in microhardness compared to the pure Ti13Zr13Nb alloy. This effect can be attributed to the reinforcement of the oxide structure by nanoparticles filling the pores. However, it should be noted that the hardness of HAp coatings is strongly correlated with their porosity and EPD voltage – studies from 2017 showed that increasing the voltage from 15V to 30V resulted in a decrease in hardness from 0.22 GPa to 0.06 GPa due to a more porous structure at higher voltage [11-16]. The observed increase in surface hardness for coatings containing nanohydroxyapatite with added silver nanoparticles can be attributed to a reinforcement effect resulting from the presence of nanophase constituents within the porous MAO layer. Nanoparticles may act as strengthening elements, limiting local deformation and enhancing the coating's resistance to mechanical loading, which is supported by literature findings [17,18].

Coatings produced after a 5-minute MAO process and then modified using the EPD method were characterized by the highest thickness (~8 μm) with low variability of 9.12%. In contrast, the lowest thickness values and the highest variability were observed for the reference layer modified only by the EPD method. The results confirm that the parameters of the MAO process, in particular its duration, have a significant impact on the growth rate and homogeneity of the oxide layer. This relationship is consistent with reports in the literature, which indicate that extending the MAO time promotes an increase in coating thickness, although this effect may saturate at longer processing times, which is associated with a change in the nature and intensity of plasma discharges. This phenomenon has been described, among others, in studies on the kinetics of MAO coating growth, where it was shown that the thickness of the layer depends on the duration of the process and the composition of the electrolyte, and that the growth rate slows down as the thickness of the coating itself increases [19]. EDS analysis revealed a high oxygen content (above 40%) along with the presence of calcium and phosphorus in the surface region, indicating their incorporation into the coating formed after the combined MAO and EPD processes. The combination of both processes enabled the utilization of the porous oxide layer formed by MAO as a substrate conducive to the deposition of calcium–phosphate phases [17,20].

The Ca/P ratio, calculated from the EDS results, was 1.23, which is lower than the stoichiometric value characteristic of hydroxyapatite (1.67), suggesting the formation of calcium phosphates with a reduced Ca/P ratio rather than stoichiometric hydroxyapatite. This indicates that the applied EPD parameters contributed to the formation of a coating with a chemical composition potentially relevant for biomedical applications [21,22]. The addition of silver, despite its low detectability in EDS analysis (0.0–0.1%), aims to provide antibacterial properties. The low detectability of silver in EDS analysis may result from the inherent sensitivity limitations of the method or from the low concentration of nanoparticles in the EPD suspension. Nevertheless, even trace amounts of silver may exhibit antibacterial activity, which is important for minimizing the risk of peri-implant infections [23]. According to previous studies, the concentration of silver released into the SBF solution from EPD coatings exceeds the bactericidal threshold (0.1 ppm) as early as after 1–3 days, while remaining below the cytotoxicity limit [11,24,25].

Longer oxidation times may lead to excessive porosity or reduced layer cohesion, whereas shorter times do not allow for sufficiently developed structures to support effective EPD coating deposition [17,26]. Microscopic analysis (SEM) revealed that the application of MAO as a preliminary step creates a developed, porous oxide structure, which serves as an ideal substrate for the mechanical anchoring of nanohydroxyapatite and silver nanoparticles deposited by the EPD method. In contrast, coatings deposited directly onto the ground substrate (Reference + EPD sample) exhibited irregular particle agglomerates with poor adhesion, whereas the hybrid MAO+EPD layers were characterized by improved continuity and cohesion. Depositing nanoHAp directly onto titanium at low voltages can lead to the formation of shrinkage cracks during heat treatment. The use of a porous MAO sublayer in the current research appears to limit this negative effect, thereby ensuring better stability of the top layer [27,11,28].

Both modification methods significantly influenced surface wettability. The water contact angle for the MAO+EPD samples dropped to values close to zero, indicating a transition of the surface to a superhydrophilic state. This phenomenon is extremely beneficial from the perspective of osteoblast adhesion and extracellular matrix production [11,29-32]. For comparison, nanoHAp coatings deposited directly onto titanium exhibited contact angles in the range of 30–47°, which also classifies them as hydrophilic; however, the porous MAO structure drastically enhances this effect through capillary action within the micropores [33]. The combined application of MAO and EPD also led to a significant increase in surface hydrophilicity, particularly for the 5-minute MAO variant. This phenomenon can be associated with the development of a porous surface structure. Reduced hydrophobicity in favor of a hydrophilic character is widely recognized as beneficial for cell adhesion and for the effective integration of implants with bone tissue [34].

A key finding of the current research is the influence of the MAO process duration on adhesion. While the 5-minute MAO variant provided acceptable adhesion (ISO 2), extending the time to 10 minutes resulted in a complete loss of adhesion (ISO 5). This suggests that the excessive thickness and porosity of the oxide layer obtained during the MAO process generate excessive internal stresses or limit the cohesion of the bond with the EPD coagulates. In the study conducted by Santiago-Medina et al. [35], the authors demonstrated that the micro-arc oxidation process drastically alters surface topography and surface energy, which directly translates into osteoblast adhesion and proliferation. A shorter treatment time (5 min) may have resulted in the formation of a coating with insufficient thickness or suboptimal porosity, which, combined with the EPD process, could lead to unfavorable interactions at the material-cell interface. The results suggest that optimizing MAO parameters is essential to avoid negative impacts on cellular metabolism. The MAO 5 min + EPD variant, which lies on the threshold of cytotoxicity according to the ISO 10993-5 standard, suggests that extending the oxidation time to 10 min is necessary to maintain full biocompatibility. This likely provides better substrate passivation and a more stable coating structure, analogous to the more favorable results observed at higher processing parameters in the literature. The analysis by Fan et al. [36] demonstrated that MAO pretreatment creates a well-developed, porous oxide structure that serves as an ideal substrate for electrophoretically deposited particles, significantly influencing the material's biocompatibility. This may suggest that the 5-minute oxidation time was insufficient to produce a sufficiently stable and developed ceramic layer. The cited publication emphasizes that the parameters of the MAO layer determine how densely the EPD coating covers the substrate. It can therefore be concluded that in

the case of the 5-minute variant, the thinner and potentially less regular oxide layer did not provide optimal anchoring for the phase deposited during the EPD process, nor did it constitute an adequate protective barrier. Only extending the MAO process to 10 minutes allowed for full cytocompatibility, which is consistent with Fan's observations indicating the crucial importance of the MAO substrate morphology for the final biological response of the hybrid system.

Conclusions

The results of this study confirm that the two-step surface modification of the Ti-13Zr-13Nb alloy combining micro-arc oxidation (MAO) and electrophoretic deposition (EPD) is an effective approach for producing bioactive coatings with improved mechanical and surface properties relevant to implant applications. The MAO process enabled the formation of a porous oxide layer enriched with calcium and phosphorus, as confirmed by EDS analysis, indicating successful incorporation of these elements into the coating structure. This structure served as an effective substrate for EPD deposition of nanohydroxyapatite with silver nanoparticles, leading to a significant increase in coating thickness and microhardness compared to the reference material. Among the investigated variants, the MAO 5 min + EPD treatment provided the most favorable balance between coating thickness, hardness, and uniformity; however, it exhibited the highest cytotoxicity. Surface wettability measurements revealed a pronounced increase in hydrophilicity after MAO and EPD treatments, accompanied by higher surface free energy values, particularly for the MAO 5 min + EPD variant. These features are considered beneficial for implant–tissue interactions. Adhesion testing demonstrated that excessive MAO treatment time negatively affects coating adherence. While the MAO 10 min + EPD variant exhibited complete loss of adhesion, the MAO 5 min + EPD coating maintained acceptable adhesion, indicating that controlled oxidation time is critical for coating durability. In summary, the MAO 5 min + EPD variant exhibited the most favorable combination of physicochemical and mechanical properties, including a bioactive coating composition, high adhesion, increased hardness, and good surface wettability. However, the cytotoxicity assessment revealed a significant reduction in cell viability, which substantially limits its potential for direct application in implantology. The obtained results indicate that, despite the high technological potential of this surface modification, further optimization of process parameters or the implementation of additional modification steps is necessary to improve biocompatibility while maintaining the advantageous functional properties.

Acknowledgments

The authors would like to thank the laboratory staff of the Faculty of Mechanical Engineering and Ship Technology, Gdańsk University of Technology, for providing instrumental support.

References

[1] Ming X., Zhang Y., Wang L., Liu Y.: Micro-Arc Oxidation in Titanium and Its Alloys: Development and Potential of Implants. *Coatings*, 13 (2023) 28-29.
[2] Ossowska A.: *Wytwarzanie, budowa i właściwości warstw tlenkowych uzyskiwanych na stopach tytanu do zastosowań biomedycznych*. Gdańsk: Politechnika Gdańska (2017) 18-21.
[3] Loch J.: *Korozyjne zachowanie się biomedycznych stopów tytanu w symulowanych roztworach fizjologicznych*. Rozprawa doktorska (2017) 22-32.
[4] Brunette D. M., Tengvall P., Textor M., Thomsen P.: Titanium in Medicine Material Science, Surface Science, Engineering, *Biological Responses and Medical Applications* (2001) 1-13.
[5] Wen X., Li Y., Zhang D., Liu X.: Micro-arc oxidation (MAO) and its potential for improving the performance of titanium implants in biomedical applications. *Frontiers in Bioengineering and Biotechnology* (2023) 18.
[6] Niinomi M., Nakai M.: Titanium-Based Biomaterials for Preventing Stress Shielding between Implant Devices and Bone. *Materials Science and Engineering* / *PMC* (2011).
[7] Ma C., Du T., Niu X, Fan Y.: *Biomechanics and mechanobiology of the bone matrix* (2022).
[8] Świeczko-Żurek B., *Biomateriały*, Wydawnictwo Politechniki Gdańskiej, Gdańsk (2009) 87-90.
[9] Jedynak B., Mierzwińska-Nastalska E.: *Tytan – właściwości i zastosowanie w protetyce stomatologicznej*. Titanium – its properties and application in prosthetic dentistry (2013) 76.
[10] Loch J., Krawiec H., Łukaszczyk A.: *Wpływ symulowanych wodnych środowisk fizjologicznych na odporność korozyjną stopów Ti6Al4V i Ti10Mo4Zr oraz ich składników stopowych* (2015) 93.
[11] Bartmański M., Cieślik B., Głodowska J., Kalka P., Pawłowski Ł., Pieper M., Zieliński A.: Electrophoretic deposition (EPD) of nanohydroxyapatite–nanosilver coatings on Ti13Zr13Nb alloy. *Ceramics International* 43 (2017) 11820-11829.
[12] Drevet R., Ben Jaber N., Fauré J., Tara A., Ben Cheikh Larbi A., Benhayoune H.: Electrophoretic deposition (EPD) of nano-hydroxyapatite coatings with improved mechanical properties on prosthetic Ti6Al4V substrates. *Surface and Coatings Technology*, 301 (2015) 94-99.
[13] Dey A., Mukhopadhyay A.K., Gangadharan S., Sinha M.K., Basu D., Bandyopadhyay N.R.: Nanoindentation study of microplasma sprayed hydroxyapatite coating. *Ceramics International*, 35 (2009) 2295-2304.
[14] Dey A., Mukhopadhyay A.K.: Evaluation of residual stress in microplasma sprayed hydroxyapatite coating by nanoindentation. *Ceramics International*, 40 (2014) 1263-1272.
[15] Saber-Samandari S., Gross K.A.: Nanoindentation on the surface of thermally sprayed coatings. *Surface and Coatings Technology*, 203 (2009) 3516-3520.
[16] Tang C.Y., Uskokovic P.S., Tsui C.P., Veljovic D., Petrovic R., Janackovic D.: Influence of microstructure and phase composition on the nanoindentation characterization of bioceramic materials based on hydroxyapatite. *Ceramics International*, 35 (2009) 2171-2178.
[17] Makurat-Kasprolewicz B., Wekwejt M., Pezzato L., Ronowska A., Krupa J., Zimowski S., Dzionk S., Ossowska A.: Effect of ultrasound on the physicochemical, mechanical and adhesive properties of micro-arc oxidized coatings on Ti13Nb13Zr bio-alloy. *Scientific Reports*, 14 (2024).
[18] Majkowska-Marzec B., Sypniewska J., Jażdżewska M., Suchwałko K., Ciecierska M., Fernandez Hernan J.P.: Influence of the micro-arc oxidation (MAO) parameters

on surface properties of hydroxyapatite and hydroxyapatite–carbon nanotube coatings formed on the Ti13Nb13Zr alloy. *Advances in Materials Science*, 3 (2025) 39-52.
[19] Jin S., Ma X., Wu R., Wang G., Zhang J., Krit B., Betsofen S., Liu B.: Advances in micro-arc oxidation coatings on Mg-Li alloys. *Applied Surface Science Advances*, 8 (2022).
[20] Jugowiec D., Łukaszczyk A., Cieniek Ł., Kowalski K., Rumian Ł., Pietryga K., Kot M., Pamuła E., Moskalewicz T.: Influence of the electrophoretic deposition route on the microstructure and properties of nano-hydroxyapatite/chitosan coatings on the Ti-13Nb-13Zr alloy. *Surface and Coatings Technology*, 324 (2017) 64-79.
[21] Latocha J.: *Procesy otrzymywania nanocząstek hydroksyapatytu o różnej morfologii do zastosowań biomedycznych*. Rozprawa doktorska, Politechnika Warszawska (2023) 19-30.
[22] Krukowski S.: Synteza i badania strukturalne hydroksyapatytów wapniowych modyfikowanych aminokwasami. *Biuletyn Wydziału Farmaceutycznego Warszawskiego Uniwersytetu Medycznego*, 11 (2013) 48-55.
[23] Sypniewska J., Pawłowski Ł., Mirowska A., Szkodo M.: Hybrid enrichment of Ti13Nb13Zr alloy with zinc ions and silver nanoparticles using a combination of micro-arc oxidation and electrophoretic deposition. *Scientific Reports*, 15 (2025) 30769.
[24] Zima A.: *Wpływ dodatków modyfikujących na właściwości hydroksyapatytowych wielofunkcyjnych tworzyw implantacyjnych przeznaczonych na nośniki leków*. Rozprawa doktorska, Akademia Górniczo-Hutnicza im. Stanisława Staszica w Krakowie (2007).
[25] Mirzaee M., Vaezi M., Palizdar Y.: Synthesis and characterization of silver-doped hydroxyapatite nanocomposite coatings and evaluation of their antibacterial and corrosion resistance properties in simulated body fluid. *Materials Science and Engineering* C, 69 (2016) 675-684.
[26] Rościszewska M.: *Wytwarzanie i modyfikacja powierzchni porowatych struktur tytanowych przeznaczonych na implanty*. Rozprawa doktorska, Politechnika Gdańska (2022).
[27] Bartmański M.: *Wytwarzanie powłok hydroksyapatytowych z osłoną biologiczną na stopie tytanu*. Rozprawa doktorska, Politechnika Gdańska (2018).
[28] Boccaccini A.R., Keim S., Ma R., Li Y., Zhitomirsky I.: Electrophoretic deposition of biomaterials. *Journal of the Royal Society Interface*, 7 (2010) 581-613.
[29] Feng B., Weng J., Yang B.C., Qu S.X., Zhang X.D.: Characterization of surface oxide films on titanium and adhesion of osteoblast. *Biomaterials*, 24 (2003) 4663-4670.
[30] Gross K.A., Babovic M.: Influence of abrasion on the surface characteristics of thermally sprayed hydroxyapatite coatings. *Biomaterials*, 23 (2002) 4731-4737.
[31] Rautray T.R., Narayanan R., Kim K.H.: Ion implantation of titanium based biomaterials. *Progress in Materials Science*, 56 (2011) 1137-1177.
[32] Boyan B.D., Hummert T.W., Dean D.D., Schwartz Z.: Role of material surfaces in regulating bone and cartilage cell response. *Biomaterials*, 17 (1996) 137-146.
[33] Heise S., Höhlinger M., Torres Y., Palacio J.J., Ortiz J.A., Wagener V., Virtanen S., Boccaccini A.R.: Electrophoretic deposition and characterization of chitosan/bioactive glass composite coatings on Mg alloy substrates. *Electrochimica Acta*, 232 (2017) 456-464.
[34] Barczyk J.: Multifunkcjonalne powłoki ceramiczne wytworzone na β-stopie tytanu do zastosowań medycznych otrzymywane metodą PS-PVD. Doctoral thesis, Uniwersytet Śląski (2022).
[35] Santiago-Medina P., Sundaram P. A., Diffoot-Carlo N.: The Effects Of Micro Arc Oxidation Of Gamma Titanium Aluminide Surfaces On Osteoblast Adhesion And Differentiation. *J Mater Sci Mater Med*. (2014) 1577-1587.
[36] Fan X., Du J., Li Y., Duan K., Liu G.: Electrophoretic deposition of magnesium oxide coating on micro-arc oxidized titanium for antibacterial activity and biocompatibility. *Journal of Orthopaedic Surgery and Research* 18 (2023) 901.
[37] Dziaduszewska, M., Shimabukuro, M., Seramak, T., Zielinski, A., Hanawa, T. Effects of Micro-Arc Oxidation Process Parameters on Characteristics of Calcium-Phosphate Containing Oxide Layers on the Selective Laser Melted Ti13Zr13Nb Alloy. *Coatings*, 10 (2020) 745.